

1-1-2021

Modelling and simulation of solar thermal power generation network

Bowen Wang
Florida International University

Follow this and additional works at: https://digitalcommons.fiu.edu/all_faculty

Recommended Citation

Wang, Bowen, "Modelling and simulation of solar thermal power generation network" (2021). *All Faculty*. 471.

https://digitalcommons.fiu.edu/all_faculty/471

This work is brought to you for free and open access by FIU Digital Commons. It has been accepted for inclusion in All Faculty by an authorized administrator of FIU Digital Commons. For more information, please contact dcc@fiu.edu.

MODELLING AND SIMULATION OF SOLAR THERMAL POWER GENERATION NETWORK

by

Bowen WANG*

Florida International University, Miami, Fla., USA

Original scientific paper
<https://doi.org/10.2298/TSCI2104905W>

In the smart grid context, the article combines SEGS-VI solar thermal power station parameters to establish a solar thermal power generation system model. The thesis is based on the First and Second laws of thermodynamics. It uses the white box model analysis method of the energy system to calculate the solar thermal power generation system-concentrating and collecting subsystem, heat exchange subsystem, and power subsystem to obtain the subsystems dissipation of each process. Finally, the article uses the white box model analysis of the total energy system to treat the subsystems as white boxes, and connects them to form a white box network, makes a reasonable evaluation of the energy consumption status of the total energy system, and finds the weak links in the energy use process of the system. Provide a basis for system energy saving.

Key words: *smart grid, solar thermal power generation, white box model, exergy calculation, exergy dissipation, modelling*

Introduction

For many years, thermal efficiency analysis has been widely used to evaluate solar thermal power systems' thermal performance. The thermal efficiency analysis method is an energy quantity analysis method based on the First law of thermodynamics. Its essence is the ratio of the thermal equipment's significant energy to the total input energy. It quantitatively reflects the level of energy used by the thermal equipment. The shortcomings of the thermal efficiency analysis method are: firstly, it cannot reflect the reasons for energy loss in the energy use process and secondly, it only analyzes the amount of energy without considering the difference in the energy quality and grade. The analysis method is a systematic method based on the First and Second thermodynamics laws, which uses efficiency to evaluate the performance of the thermal system and the perfection of the thermal cycle. The efficiency analysis method's essence is to comprehensively consider the utilization degree of energy in two aspects: quantity and quality [1]. The solar thermal power generation system adopts an efficiency analysis method to comprehensively and reasonably evaluate the system's thermal performance and perfection. Through the analysis of the white-box model, the efficiency of each subsystem of the solar thermal power generation system is calculated, and the available power of the entire system is analyzed to determine the amount and location of the loss and find the weak links of energy use to provide a basis for system energy saving.

* Author's e-mail: bowenwang4291@163.com

Solar thermal power generation system model

The basic working principle of solar thermal power generation is to combine trough-shaped parabolic concentrating heat collectors in series and parallel, using trough-shaped parabolic mirrors to focus the sunlight on the linear receiver installed at the focus point of the parabolic mirror and convection through the receiver. The heat medium is heated, and the heat medium that obtains heat energy generates high temperature and high pressure steam in the heat exchanger, which drives the conventional steam turbine generator set to generate electricity. Based on this, the solar thermal power generation system model is established. The solar thermal power generation system model adopts a double loop cycle, including a heat transfer oil loop and a steam loop [2]. The system is divided into concentrating and heat collecting subsystem, heat exchange subsystem, and power subsystem, fig. 1.

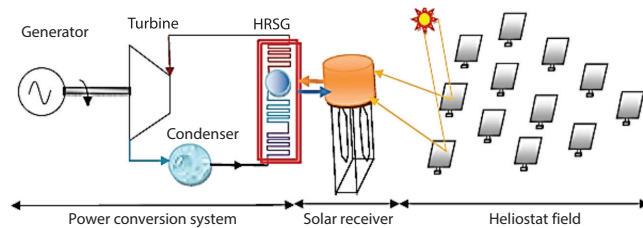


Figure 1. Solar thermal power generation system model

The system's first loop is composed of a solar mirror field, liquid heat transfer oil HTF, expansion tank, pump, and heat exchanger. The solar energy is radiated to the mirror field and converted into heat transfer oil HTF through the concentrating heat collector. After the HTF obtained by the system passes through the expansion tank, part of it passes through the superheater, steam generator, and preheater to heat the main steam, and the other part enters the reheater to heat the exhaust stream of the high pressure cylinder of the steam turbine. The HTF at the preheater and reheater outlet is pumped to the concentrating heat collector and heated to form a circulation. The second loop of the system is consistent with the traditional Rankine cycle.

Exergy analysis of concentrating and collecting subsystem

We know that the average surface temperature of the Sun is $t_a = 5490$ °C, the direct irradiance $I = 875$ W/m², the incident angle is 0° , and the ambient temperature $t_0 = 20$ °C. The sun's radius is $R = 6.963 \cdot 10^5$ km, and the distance between the Sun and the Earth is $D = 1.471 \cdot 10^8$ km. The collector area of the SEGS-VI system collector is 193200 m². Concentrating and collecting subsystems include optical loss and thermal energy loss to convert solar energy into heat. The optical loss mainly occurs in the mirror field and the collector, and the thermal exergy loss mainly occurs when converting solar energy to thermal energy. The exergy calculation results of the condenser and heat collection subsystem are shown in tab. 1. The white box model of the condenser and heat collection subsystem is shown in fig. 2. The dotted line in the white box model represents the system surrounded by *transparent* boundaries. The exergy flow lines with arrows indicate the flow of input and output. The black dots represent external exergy loss, and the white dots represent internal exergy loss [3].

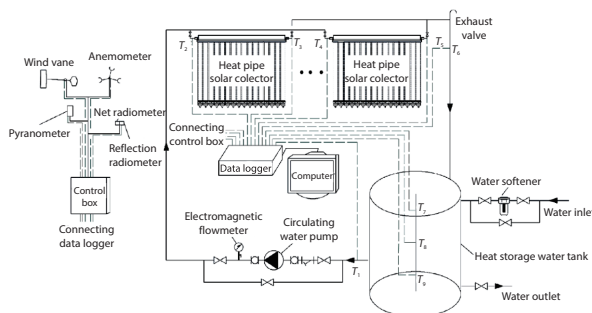


Figure 2. White box model of the condenser and heat collection subsystem

The exergy calculation results of the condenser and heat collection subsystem are shown in tab. 1. The white box model of the condenser and heat collection subsystem is shown in fig. 2. The dotted line in the white box model represents the system surrounded by *transparent* boundaries. The exergy flow lines with arrows indicate the flow of input and output. The black dots represent external exergy loss, and the white dots represent internal exergy loss [3].

Table 1. Calculation results of the condenser and heat collection subsystem

E_1 [kW]	E_2 [kW]	E_3-E_4 [kW]	E_5 [kW]	E_6 [kW]	η_{ex} [%]	λ_s [%]	λ_{At} [%]
160455	45986	42044	72425	114469	26.20	28.66	45.14

It can be seen from fig. 2 that the internal loss of the light-concentrating and heat-collecting subsystem is heat loss, E_5 , and the external loss is optical loss, E_2 . Table 1 shows that the system's exergy efficiency is 26.20%, and the weak link in the heat exergy loss.

Exergy analysis of heat exchange subsystem

The surrounding environment of the system is the baseline state of exergy analysis. When the ambient temperature is 20 °C, the specific enthalpy of air is $h_o = 295.41$ kJ/kg. According to the system's SEGS-VI design parameters, the main parameters of the fluid obtained are shown in tab. 2. The heat exchange subsystem transfers the heat energy of the HTF to water/steam, and the unit equipment constituting the heat exchange subsystem includes a superheater, a steam generator, and a preheater [4].

Table 2. The main parameters of the fluid

Project	Preheater		Steam generator	
	Import	Export	Import	Export
HTF temperature [°C]	323.9	303	373.92	323.9
HTF flow [kgs ⁻¹]	–	–	345	–
Water/steam temperature [°C]	234.83	311	311	311
Water/steam flow rate [kgs ⁻¹]	–	–	32.62	–
Enthalpy of water/steam [kW]	1014.8	1408.3	1407.2	2727.64
Project	Superheater		Reheater	
	Import	Export	Import	Export
HTF temperature [°C]	385.57	373.92	385.57	262.7
HTF flow [kgs ⁻¹]	–	–	–	44.7
Water/steam temperature [°C]	311	371	208.7	372
Water/steam flow rate [kgs ⁻¹]	–	–	–	27.85
Enthalpy of water/steam [kW]	2724.46	3005	2709.6	3190

According to the knowledge of engineering thermodynamics, the heat exchange formula between the heat exchanger and the environment:

$$Q_{xi} = \dot{m}_x (h_{xi} - h_o) \quad (1)$$

where Q_{xi} is the maximum heat transfer amount when the fluid-flows through the inlet and outlet of the heat exchanger, \dot{m}_x – the mass-flow rate of the fluid when the fluid-flows through the inlet and outlet of the heat exchanger, h_{xi} – the specific enthalpy of the fluid passing through the heat exchanger, and x, i, and o are subscript the fluid; i, inlet and outlet of the heat exchanger:

$$E_{xi} = Q_{xi} \left(1 - \frac{T_o}{T_{xi}} \right) \quad (2)$$

where E_{xi} is the heat energy when the fluid-flows through the inlet and outlet of the heat exchanger and T_{xi} – the temperature when the fluid-flows through the inlet and outlet of the heat

exchanger. The irreversible loss caused by the temperature difference heat transfer of the two heat transfer media, water vapor and HTF in the heat exchanger $E_{L,i}$. The calculation formula for the irreversible loss of the heat exchanger:

$$E_{L,i} = (E_{H1} - E_{H2}) - (E_{S2} - E_{S1}) \quad (3)$$

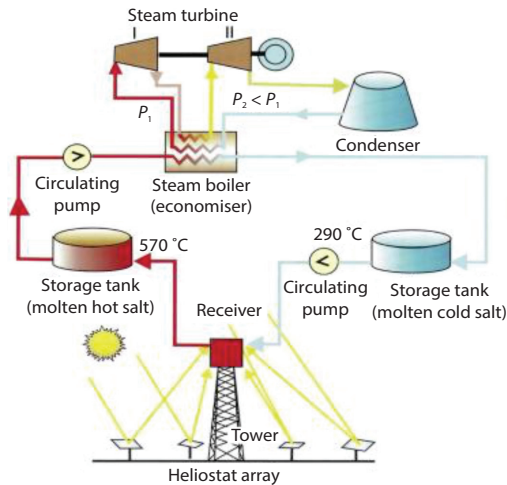


Figure 3. White box model

where E_{H1} , E_{H2} are the HTF inlet and outlet exergy and E_{S2} , E_{S1} – the water vapor inlet and outlet exergy. We build the white-box model of the heat exchanger, as shown in fig. 3. The dotted line in the figure represents the heat exchanger system enclosed by a transparent boundary. The inlet water vapor E_{S1} of the system is taken in, and the outlet water vapor E_{S2} is output. Import HTFEH1 is for supply, and export HTFEH2 is invalid. Invalidity is an external loss. The irreversible loss $E_{L,i}$ is internal [5]. Since the heat dissipation loss of the superheater system is minimal, it can be ignored.

The balanced equation of the white-box model of the heat exchanger system:

$$E_{H1} + E_{S1} = E_{H2} + E_{S2} + E_{L,i} \quad (4)$$

The efficiency of the heat exchanger:

$$\eta_{ex} = \frac{E_{S2} - E_{S1}}{E_{H1} - E_{H2}} \quad (5)$$

The thermodynamic perfection e of the heat exchanger:

$$e = \frac{E_{S2} + E_{H2}}{E_{H1} + E_{S1}} \quad (6)$$

The loss coefficient of the irreversible process of the heat exchanger:

$$\lambda_{At} = \frac{E_{L,i}}{E_{H1}} \quad (7)$$

Analysis of the superheater

According to the inlet and outlet temperature values of the superheater in tab. 2, check the characteristics of the heat transfer oil, the specific enthalpy of the inlet and outlet of the heat transfer oil are $h_1 = 770.53$ kJ/kg and $h_2 = 731.00$ kJ/kg, respectively. From eq. (1), the maximum heat output of HTF at the inlet and outlet of the superheater is $Q_{H1} = 164054$ kW and $Q_{H2} = 150279$ kW, respectively. The maximum heat release that water vapor can have is $Q_{S1} = 79235$ kW and $Q_{S2} = 88387$ kW, respectively.

From eq. (2), the HTF values of the inlet and outlet of the superheater are $E_{H1} = 91065$ kW and $E_{H2} = 81800$ kW. The values of water vapor are $E_{S1} = 39482$ kW and $E_{S2} = 48173$ kW, respectively.

From eq. (3), the irreversible loss of the two fluids in the superheater during the heat transfer process is $E_{L,i} = 574$ kW. Calculated by eq. (5), the efficiency of the superheater

is $\eta_{ex} = 93.8\%$. Calculated by eq. (6), the thermodynamic perfection of the superheater is $e = 99.56\%$. Calculated by eq. (7), the heat loss coefficient of the superheater is $\lambda_{At} = 0.63\%$.

Analysis of steam generator

According to the import and export parameters of the steam generator in tab. 2, the inlet and outlet temperature of the heat transfer oil is $t_1 = 373.92\text{ }^\circ\text{C}$, $t_2 = 323.90\text{ }^\circ\text{C}$, and the heat transfer oil characteristics table is $h_1 = 731.00\text{ kJ/kg}$, $h_2 = 617.06\text{ kJ/kg}$. Ignoring the heat loss, the steam generator's HTF inlet value is the superheater outlet's HTF value, which is $E_{HI} = 81800\text{ kW}$. From eqs. (1) and (2), the steam generator HTF outlet value is $E_{H2} = 58847\text{ kW}$, the inlet water value is $E_{S1} = 18071\text{ kW}$, and the outlet steam value is $E_{S2} = 39509\text{ kW}$.

From eq. (3), the irreversible loss of the two types of bodies in the steam generator during the heat transfer process $E_{L,i} = 1515\text{ kW}$. Calculated by eq. (5), the efficiency of the steam generator is $\eta_{ex} = 93.40\%$. Calculating from eq. (6), the thermodynamic perfection of the steam generator $e = 98.48\%$. From eq. (7), the steam generator's heat loss coefficient can be calculated as $\lambda_{At} = 1.85\%$.

Analysis of the preheater

In the same way, according to the inlet and outlet parameter values of the preheater in tab. 2, the inlet and outlet temperature of the heat transfer oil is $t_1 = 323.90\text{ }^\circ\text{C}$, $t_2 = 309\text{ }^\circ\text{C}$, check the heat transfer oil characteristics table, $h_1 = 617.06\text{ kJ/kg}$, $h_2 = 581.56\text{ kJ/kg}$. Neglecting the heat loss, the HTF inlet value of the preheater is the HTF value of the steam generator outlet, which is $E_{HI} = 58847\text{ kW}$. From eqs. (1) and (2), the HTF outlet value of the preheater $E_{H2} = 49021\text{ kW}$, the inlet water value $E_{S1} = 9927\text{ kW}$, and the outlet water vapor value $E_{S2} = 18089\text{ kW}$. From eq. (3), the irreversible loss of the two fluids in the preheater during the heat transfer process is $E_{L,i} = 1664\text{ kW}$. Calculated by eq. (5), the efficiency of the preheater is $\eta_{ex} = 83.07\%$. Calculated by eq. (6), the thermodynamic perfection of the preheater is $e = 97.58\%$. Calculated by eq. (7), the heat loss coefficient of the preheater is $\lambda_{At} = 2.83\%$.

The heat exchanger white-box model's analysis results show that the significant losses of the superheater, steam generator, and preheater are irreversible $E_{L,i}$. From the calculation results, the preheater's irreversible loss coefficient is the largest, and efficiency is the lowest, which is 83.07%. The thermodynamic perfection is also lower than that of the superheater and steam generator, but not much different [6]. The efficiency of the superheater and steam generator is higher, both above 90%.

The white box model of heat exchange subsystem

When the heat exchange subsystem transfers HTF's thermal energy to water/steam, there are irreversible losses E_{L1} caused by temperature difference heat transfer and losses E_{L2} caused by friction in the superheater, steam generator, and preheater. These losses are collectively referred to as the internal loss E_{11} of the heat-exchange subsystem. The white box model of the heat exchange subsystem is shown in fig. 3. It can be seen from fig. 3 that the supply of the heat exchange subsystem is E_3 when HTF flows into the superheater; the input of the subsystem is the feed water E_8 flowing into the preheater; the internal loss of the subsystem is the sum of irreversible loss and friction loss E_9 . The effectual output of the subsystem it is the water vapor output E_7 of the superheater; the invalidity of the subsystem is the HTF output E_4 of the preheater. Then the balance equation of the heat exchange subsystem:

$$E_3 + E_8 = E_4 + E_7 + E_9 \quad (8)$$

From eq. (8), the internal loss $E_9 = 3798$ kW can be obtained.
The efficiency of the heat exchange subsystem:

$$\eta_{\text{ex}_2} = \frac{E_7 - E_8}{E_3 - E_4} \times 100\% = 90.97\% \quad (9)$$

The white box model's analysis shows that the efficiency of the heat exchange subsystem is high, but there is still inevitably irreversible loss caused by temperature difference heat transfer [7].

Analysis of the power subsystem

The power subsystem uses the traditional Rankine cycle. The regenerative system is *two highs, three lows, and one deaeration*. The steam turbine unit's six-stage extraction steam share and the conversion efficiency of the steam turbine unit are shown in tab. 2. According to the water/steam parameters in tab. 2, the steam exchange heat, Q , of the mainstream in the heat exchanger and reheater can be calculated. The heat transfer formula of steam in the heat transfer process of the heat exchanger:

$$Q_i = \dot{m}_s \Delta h \quad (10)$$

where Q_i is the heat exchange rate of steam and \dot{m}_s – the mass-flow of water vapor.

From eq. (10), we can get the superheater steam heat exchange heat $Q_1 = 9151$ kW, the steam generator steam heat exchange heat $Q_2 = 43073$ kW, the preheater steam heat exchange heat $Q_3 = 12836$ kW, and the reheater steam heat exchange heat $Q_4 = 13369$ kW. The total steam heat exchange Q [kW]:

$$Q = Q_1 + Q_2 + Q_3 + Q_4 = 78429 \quad (11)$$

The shaft power, W_s [kW], output by the steam turbine:

$$W_s = Q\eta_e = 29803 \quad (12)$$

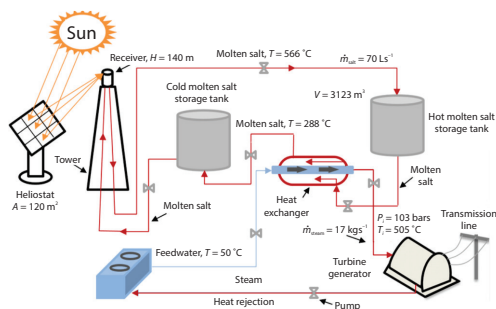


Figure 4. White box model of the power subsystem

The white box model of the power subsystem is shown in fig. 4. It can be seen from fig. 4 that due to the shaft power grade $A_s = 1$, the effectual output of the power subsystem is $E_{10} = W_s = 29803$ kW. The output of the superheater water vapor supplied by the subsystem is $E_7 = 48173$ kW. The internal loss of the subsystem is E_1 . The invalid of the preheater feed water $E_8 = 9927$ kW.

Then the balance equation of the dynamic subsystem:

$$E_7 = E_8 + E_{10} + E_{11} \quad (13)$$

From eq. (13), the internal loss $E_{11} = 8443$ kW can be obtained.

The efficiency of the power subsystem:

$$\eta_{\text{ex}_3} = \frac{E_{10}}{E_7 - E_8} \times 100\% = 77.92\% \quad (14)$$

The white box model's analysis shows that the efficiency of the power subsystem is 77.92%, the internal loss is 8443 kW, and the external loss is 9927 kW. Both losses are rela-

tively large, which is the main factor causing the reduction of the system's available power. Besides improving efficiency, steam turbine units' conversion efficiency also needs to be further improved [8].

Analysis of solar thermal power generation system

From the aforementioned analysis, the efficiency of the system:

$$\eta_{ex} = \eta_{ex_1} \eta_{ex_2} \eta_{ex_3} = 18.57\% \quad (15)$$

The total loss of the system:

$$E = E_1 - E_{10} = 130652 \text{ kW} \quad (16)$$

We establish the white-box model of the solar thermal power generation system, regard the subsystems in the system as white boxes, and connect them to form a white box network, as shown in fig. 5. The solar thermal power generation system's efficiency is only 18.57%, and the loss is as high as 130652 kW, accounting for 81.42% of the total input. From the perspective of the efficiency and loss of the subsystem, the system utilization's weak point is the light-concentrating and heat-collecting subsystem, whose efficiency is only 26.20%, and the loss accounts for 73.80% of the input. Therefore, if we want to improve the overall system's efficiency, the key is to reduce the loss of the condenser and heat collection subsystem and improve its efficiency. Secondly, the power subsystem's efficiency is 77.92%, and the loss accounts for 22.22% of the input. The heat exchange subsystem's efficiency is 90.97%, and the loss accounts for 9.03% of the input.

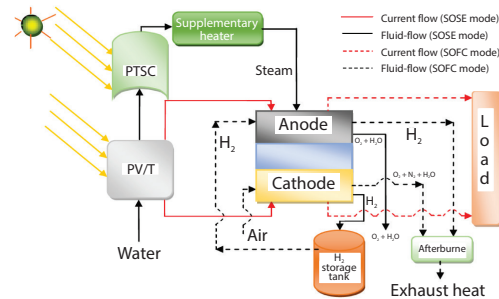


Figure 5. White box model of the solar thermal power generation system

Conclusion

The solar thermal power generation system's efficiency is 18.57%, and the total loss of the system accounts for 81.42% of the total input. It can be seen that the energy utilization rate of the system is meager, and the energy loss is profound. We calculated that the condenser and heat collection subsystem's efficiency was 26.20%, the efficiency of the heat exchange subsystem was 90.97%, and the efficiency of the power subsystem was 77.92%. Therefore, the weak link in the solar thermal power generation system utilization lies in the light collection and heat collection subsystem. Therefore, the key to improving the system's energy utilization rate is to improve the efficiency of the concentrating and heat collecting subsystem. Secondly, the power subsystem's efficiency needs to be further improved, mainly by improving the water vapor parameters and the conversion efficiency of the steam turbine unit. The light collecting and heat collecting subsystem is the weak link of the overall system utilization. In the loss of the light-concentrating and heat-collecting subsystem, the optical loss coefficient is 28.66%, and the heat loss coefficient is 45.14%. It can be seen that both losses are large, and the heat loss is the weak link of the concentrating and collecting subsystem. Therefore, when reducing these two types of losses, emphasis should be placed on reducing heat loss. The efficiency of the heat exchange subsystem is higher, 90.97%. Among them, the superheater's efficiency is 93.80%,

the efficiency of the steam generator is 93.40%, and the efficiency of the preheater is 83.07%. It can be seen that the loss of the preheater in the heat exchanger is more, which is the weak link in the energy use of the heat exchange subsystem.

References

- [1] Deng, Z., *et al.*, The Emergence of Solar Thermal Utilization: Solar-Driven Steam Generation, *Journal of Materials Chemistry A*, 15 (2017), 17, pp. 7691-7709
- [2] Ranjan, S., *et al.*, Parabolic trough Solar-Thermal-Wind-Diesel Isolated Hybrid Power System: Active Power/Frequency Control Analysis, *IET Renewable Power Generation*, 12 (2018), 16, pp. 1893-1903
- [3] Wu, S., Study and Evaluation of Clustering Algorithm for Solubility and Thermodynamic Data of Glycerol Derivatives, *Thermal Science*, 23 (2019), 5, pp. 2867-2875
- [4] Saleem, M. S., *et al.*, Design and Optimization of Hybrid Solar-Hydrogen Generation System Using TRNSYS, *International Journal of Hydrogen Energy*, 45 (2020), 32, pp. 15814-15830
- [5] Xu, C., *et al.*, Research Progress on Novel Solar Steam Generation System Based on Black Nanomaterials, *The Canadian Journal of Chemical Engineering*, 96 (2018), 10, pp. 2086-2099
- [6] Choi, K., *et al.*, Influence of Temperature Gradient Induced by Concentrated Solar Thermal Energy on the Power Generation Performance of a Thermoelectric Module, *Journal of the Korea Academia-Industrial Cooperation Society*, 18 (2017), 10, pp. 777-784
- [7] Duan, L., *et al.*, Performance Analysis of a Tower Solar Collector-Aided Coal-Fired Power Generation System, *Energy Science & Engineering*, 5 (2017), 1, pp. 38-50
- [8] Wu, S., Construction of Visual 3-D Fabric Reinforced Composite Thermal Performance Prediction System, *Thermal Science*, 23 (2019), 5, pp. 2857-2865